

# Seasonal Variations of the Earth's Gravitational Field: An Analysis of Atmospheric and Ocean Tidal Excitation

D. Dong, R. S. Grins, J. O. Dickey

Space Geodetic Science and Applications Group

Jet Propulsion Laboratory, California Institute of Technology, Pasadena, California

*Abstract.* Laser ranging measurements to a single satellite are sensitive to the Earth's gravitational field and its temporal variations. Using 13 years (1980-1992) of LAGEOS I laser ranging data, we have recovered monthly mean linear combinations of even and odd degree zonal spherical harmonic coefficients of the Earth's gravitational field. Because unmodeled once-per-revolution accelerations of LAGEOS I of currently unknown origin contaminate the recovered odd degree zonal gravitational field coefficients, we focus our attention in this report on the even combination which exhibits a significant secular trend as well as dominant seasonal variations (at annual and semi-annual periods). Comparing this observed result with the same linear combination of even zonal spherical harmonic coefficients derived from gridded global surface pressure data of the National Meteorological Center (NMC) from 1984 to 1992 indicates that atmospheric pressure fluctuations are the dominant cause of the observed even zonal gravitational field variations at the annual period, explaining the observed amplitude to within  $1\sigma$  and the phase to within  $20^\circ$ . At the semi-annual period, the modeled effect of the self-consistent equilibrium ocean tide is found to be greater than that of atmospheric pressure fluctuations, with agreement with the observations seen at the  $1\sigma$  level when both effects are considered. The influence of seasonal variations in groundwater is also discussed.

## 1. INTRODUCTION

The Earth is a dynamic system— it has a fluid, mobile atmosphere and oceans, a continually changing global distribution of ice, snow, and ground water, a fluid core that is undergoing some type of hydromagnetic motion, a mantle both thermally convecting and rebounding from the glacial loading of the last ice age, and mobile tectonic plates. These processes affect a number of global geodynamic properties of the Earth including its gravitational field, rotation, and location of the Earth's center-of-mass relative to the crust. Since the gravitational field of the Earth changes only in response to net mass redistributions, observations of the Earth's time varying global gravitational field allow the isolation and subsequent investigation into the changing mass distribution of the Earth (see

for example, *Yoder et al., 1983; Rubincam, 1984; Cheng et al., 1989; Nerem et al., 1993; Gegout and Cazenave, 1993*). Here, we investigate seasonal variations in the Earth's gravitational field through the analysis of LAGEOS 1 satellite laser ranging (SLR) measurements spanning 1980 to 1992. Global surface pressure data from the National Meteorological Center (NMC) spanning 1984 to 1992 are analyzed to study the contribution of atmospheric mass redistributions to the observed variations of the Earth's gravitational field, in addition, a self-consistent equilibrium ocean tide model [*Ray and Cartwright, 1994*] is used to predict the contribution of the annual and semi-annual ocean tides to the observed seasonal gravitational field variations, and the contribution of seasonal groundwater variations is also considered. Since laser ranging measurements to a single satellite are only sensitive to certain satellite-dependent linear combinations of the even and, separately, odd degree zonal gravitational field coefficients, we form those same linear combinations of coefficients when modeling the effect on the gravitational field of seasonal atmospheric pressure, ocean tidal, and groundwater variations.

## 2. DATA ANALYSIS

We analyze LAGEOS I laser ranging measurements acquired during 1980-1992 utilizing the GODYN software package to perform numerical integration of satellite orbits and to construct normal matrices for every monthly orbit segment. The a priori models adopted in determining the LAGEOS 1 orbit are: Wahr's solid Earth tide model, an equilibrium model for the 18.6 year tide [*Trupin and Wahr, 1990*], the JGM-2 gravitational field model [*Nerem et al., 1994b*] and its corresponding ocean tide model. Since both the annual (Sa) and semi-annual (Ssa) tides of the JGM-2 ocean tide model are contaminated by the effects of annual and semi-annual fluctuations in atmospheric mass distribution, we set to zero the zonal Sa and Ssa ocean tide amplitudes through spherical harmonic degree 8 in order to fully remove from the a priori model the contributions of seasonal atmospheric pressure and ocean tide variations. The effects of solar radiation pressure, albedo, atmospheric drag, and Yarkovsky thermal drag [*Rubincam, 1988*] are included. General relativistic corrections [*Huang et al., 1990*] are taken into account and the DE200 planetary ephemeris is adopted. The JGM-2 model related site coordinates and velocities are held fixed, and the geometrical corrections of site positions due to solid Earth tide and ocean tide loading [*Scherneck, 1991*] are employed. The SPACE92 Earth orientation series [*Gross, 1993*] was adopted to provide Universal Time (UT1-TAI) and polar motion.

The considered parameters in our analysis include satellite state vectors every 30 days with along-track acceleration parameters solved for every 15 days, monthly-averaged

normalized geopotential spherical harmonic coefficients through degree and order 8 are determined at monthly intervals. In total, 85 parameters are considered for each month-long interval. Note that since ranges to a single satellite are only capable of determining certain linear combinations of the gravitational field coefficients, we impose a general mapping function [Dong and Bock, 1989] to each normal matrix to project the 77 considered geopotential coefficients onto 4 independent parameters. In this study, the chosen independent parameters are 1 linear combinations of the even and, separately, the odd degree zonal gravitational field coefficients, as well as two additional linear combinations of the non-zonal coefficients.

The effect of surface mass variations on the Earth's global gravitational field as parameterized by the fully normalized gravitational field coefficients ( $C_{lm}, S_{lm}$ ; also known as the Stokes coefficients) can be shown to be [e.g., Chao, 1994]:

$$\begin{aligned} C_{lm} &= \frac{1 + k_1'}{21 - I} \frac{R_e^2}{M} \int_S q(\varphi, \lambda) \frac{\cos(m\lambda)}{\sin(m\lambda)} P_{lm}(\sin \varphi) dS \\ S_{lm} &= \frac{1 + k_1'}{21 - I} \frac{R_e^2}{M} \int_S q(\varphi, \lambda) \frac{\sin(m\lambda)}{\sin(m\lambda)} P_{lm}(\sin \varphi) dS \end{aligned} \quad (1)$$

where  $M$  is the mass of Earth,  $R_e$  is the radius of the Earth,  $k_1'$  is the load Love number of degree 1,  $\varphi$  is the latitude,  $\lambda$  is the longitude, and  $P_{lm}(\sin \varphi)$  are normalized Legendre functions with the integral of  $P_{lm}^2(\sin \varphi)$  over the surface of a sphere equal to  $4\pi$ . In this study, we set  $k_2' = -0.308$ ,  $k_4' = -0.132$ ,  $k_6' = -0.089$  and  $k_8' = -0.078$  [Farrel, 1972]. The surface load mass density is denoted by  $q(\varphi, \lambda)$ . For the case of surface pressure loading,  $q(\varphi, \lambda) = p(\varphi, \lambda)/g$ , while for ocean tide loading,  $q(\varphi, \lambda) = \rho_w h(\varphi, \lambda)$ . Here,  $g$  is the gravitation] acceleration,  $\rho_w = 1025 \text{ kg/m}^3$  is the ocean water density, and  $h(\varphi, \lambda)$  is the ocean tide height (set to zero over land).

The NMC gridded global surface pressure data used here spans 1984-1992 at 12-hour intervals with a spatial resolution of  $2.5^\circ \times 2.5^\circ$ . The atmospheric coefficients at each 12-hour interval are calculated for both the non-inverted barometer (NIB) and inverted barometer (IB) models for the response of the oceans to atmospheric pressure variations. The NIB model treats the ocean as a rigid body thereby fully transmitting the imposed surface loading to the underlying oceanic crust. On the other hand, the IB model considers the ocean's response to surface loading as purely isostatic. The response of the real ocean is likely to be somewhere between these two extremes. Using (1), we calculate the atmospheric pressure-induced zonal gravitational field coefficients to degree 8 and form monthly means over the same time intervals as the LAGEOS solutions. For comparison

with the I-AGP;OS-observed gravitational field coefficients, the same linear combination of the even zonal harmonics (see following sections) are formed using the monthly means of the atmospheric geopotential coefficients for both the 1 B and N1B cases.

### 3. RESULTS AND COMPARISONS

By definition, the linear combinations of the even and, separately, odd gravitational field coefficients are given by:

$$C_{\text{even}} = C_{20} + a_4 C_{40} + a_6 C_{60} + a_8 C_{80} + \dots \quad (2)$$

$$C_{\text{odd}} = C_{30} + a_5 C_{50} + a_7 C_{70} + \dots$$

Here  $a_4, a_5, \dots, a_8$  are the linear combination coefficients. The observed monthly  $C_{\text{even}}$  and  $C_{\text{odd}}$  solutions recovered from the LAGEOS I satellite laser ranging measurements spanning 1980 - 1992 are plotted in Figure 1. To focus on the temporal variations of the gravitational field, we have removed the mean values from the monthly  $C_{\text{even}}$  and  $C_{\text{odd}}$  solutions. For the  $C_{\text{even}}$  series, the dominant structures are the annual and semi-annual variations with a significant secular trend and some indication of interannual variations. For the  $C_{\text{odd}}$  series, the dominant structures are annual variations with the so-called "LAGEOS anomaly" [Eanes and Watkins, 1991] appearing in 1989, 1991 and 1992. These apparently anomalous variations in the estimated  $C_{\text{odd}}$  series are thought to be caused by unmodeled once-per-revolution perturbation forces, to which the LAGEOS orbital eccentricity is very sensitive. Recent study [Nerem et al., 1994a] suggests that the "LAGEOS anomaly" may be linked to perturbations caused by the atmospheric thermal tide ( $S_1$ ), which is not considered in this study. Since the "missing" unmodeled perturbation forces appear to be predominant in the  $C_{\text{odd}}$  series and are still under investigation, we will focus our discussion here on the  $C_{\text{even}}$  series.

The trend of the  $C_{\text{even}}$  estimates from 1980 to 1992 is  $1.33 \pm 0.16 \times 10^{-1}$  1/year, which is consistent with previous results at the one  $\sigma$  level and is attributable to the effects of postglacial rebound [Yoder et al., 1983; Rubincam, 1984; Cheng et al., 1989; Eanes and Watkins, 1991; Gegout and Cazenave, 1991; Nerem et al., 1993]. To obtain seasonal variations of the  $C_{\text{even}}$  estimates, we first apply a high-pass filter with a period cutoff of 2 years. From 1984 to 1992 (the interval of the available NMC atmospheric pressure data), the amplitudes of the annual and semi-annual variations of  $C_{\text{even}}$  are  $1.10 \pm 0.09 \times 10^{-10}$  and  $0.92 \pm 0.09 \times 10^{-10}$ , respectively (see Table 1). For the 1980-1989 time period, our annual amplitudes and phases as well as the semi-annual phase are in agreement at the one

Table 1

$C_{\text{even}}$ from LAGEOS	Annual variation		Semiannual variation	
	amp ( $10^{-10}$ )	phase (deg)	amp (10-10)	phase (deg)
1984-1992	1.10 (0.09)	28.6 (4,8)	0.92 (0.09)	114.9 (5.6)
1980-1989	1.13 (0.09)	27.8 (4.9)	0.94 (0.09)	111.0 (5.8)
1980-1989 ( <i>Nerem et al.</i> )	1.20	25	1.13	108

The base is relative to January 1, The numbers in parentheses represent  $1\sigma$  formal uncertainties.

$\sigma$  level with the results of *Nerem et al. [1993]* with the amplitude of our semi-annual estimate being smaller than theirs by two  $\sigma$  (Table 1).

Figure 2 compares the  $C_{\text{even}}$  linear combination of even degree zonal gravitational field coefficients recovered from LAGEOS 1 laser ranging measurements with just the  $C_{20}$  coefficients estimated from the NMC global pressure data for both the NIB and IB models. In this comparison, the low frequency components with periods longer than 2 years have been removed. The amplitudes and phases of the annual and semi-annual variations are listed in Table 2; both visual and numerical comparisons, especially of the annual amplitude, indicate a marginal preference for the NIB model. For the semi-annual variations, the  $C_{20}$  atmospheric pressure-induced geopotential amplitudes of both the NIB and IB models are only 10% of the observed  $C_{\text{even}}$  linear combination with about  $60^\circ$  phase differences. Thus, the direct comparison of the observed  $C_{\text{even}}$  linear combination with the atmospheric pressure-induced  $C_{20}$  is in conflict with the expectation that on seasonal and longer time scales the ocean's response to surface loading is close to the IB model [*Trupin and Wahr, 1990*].

The problem here, of course, is that this comparison was done between a linear combination of the observed even degree zonal gravitational field coefficients with just the second degree zonal coefficient of the modeled atmospheric pressure-induced gravitational field. The contributions from higher degree ( $l = 4, 6, \dots$ ) even zonal coefficients of the atmospheric pressure-induced gravitational field must be taken into account by forming that same linear combination of them to which laser ranging measurements to the LAGEOS I

Table 2: Variations of even zonal gravitational field from atmosphere, groundwater and ocean in comparison with the recovered geopotential coefficients from LAGEOS I. The base is relative to January 1, 1984 in sine convention.  $C_{even}$  of groundwater variations is constructed using the second and fourth degree gravitational coefficients of *Chao and O'Connor* [1988]. Both  $S_a$  and  $S_{sa}$  oceanic tidal contributions are combinations of the second to eighth even degree spherical harmonics. The numbers in parentheses represent  $1\sigma$  uncertainties. For LAGEOS I solutions, the numbers come from the formal uncertainties. For NMC solutions, the numbers are estimated from scatter analysis.

(a) Annual variation

1984-1992	amp ( $10^{-10}$ )		phase (deg)	
LAGEOS	1.10 (0.09)		28.6 (4.8)	
ocean tide $C_{even}$	0.09		267.7	
NMC $C_{20}$ only	0.98(0.10)(IWR)	0.66(0.07) (IB)	5.2 (5.8) (NIB)	26.2(6.4) (IB)
NMC $C_{even}$	1.32(0.15)(NID)	1.01(0.11) (IB)	6.0 (6.5) (NIB)	16.5(6.4) (IB)
at mos+tide	1.31 (NIB)	0.98 (IB)	2.1(NIB)	11.5 (IB)
ground water $C_{even}$	0.63		59.3	
atmos+tide+water	1.73 (NIB)	1.48 (IB)	19.9 (NIB)	29.9 (IB)

(b) Semiannual variation

1984-1992	amp ( $10^{-10}$ )		phase (deg)	
LAGEOS	0.92 (0.09)		114.9 (5.6)	
ocean tide $C_{even}$	0.55		110.7	
NMC $C_{20}$ only	0.09(0.10)(NIB)	0.09(0.07) (IB)	77.6(63.0)(NIB)	170.1 (46.9)(IB)
NMC $C_{even}$	2.42(0.15)(NIB)	0.28(0.11) (IB)	06.6(20.6)(NIB)	118.5(23.4)(IB)
atmos+tide	0.97 (NIB)	0.83 (IB)	108.9 (NIB)	113.3 (IB)
ground water $C_{even}$	0.26		266.3	
at mos+tide+water	0.74 (NIB)	0.61 (NIB)	116.7 (NIB)	124.5 (IB)

satellite are sensitive [*Yoder et al.*, 1983; *Gutierrez and Wilson*, 1987; *Cheng et al.*, 1989; *Chao and Au*, 1991]. The appropriate values to be used for the linear combination

coefficients can be determined by first noting that perturbations to the even degree zonal gravitational field coefficients of the Earth primarily affect the rate of change of the longitude of the ascending node ( $d\delta\Omega/dt$ ) of the satellite's orbit [Yoder *et al.*, 1983]. From first order orbital perturbation theory we have [Kaula, 1966; Yoder *et al.*, 1983; Gutierrez and Wilson, 1987; Cheng *et al.*, 1989]:

$$\frac{\partial \delta\Omega}{\partial t} = A (\delta C_{20} + f_4 \delta C_{40} + f_6 \delta C_{60} + \dots) \quad (3)$$

where  $A = \frac{3\sqrt{5}}{2} n \left(\frac{R_e}{a}\right)^2 \frac{\cos i}{(1 - e^2)^2}$

$$f_4 = \frac{3\sqrt{5}}{64} \left(\frac{R_e}{a}\right)^2 (7\sin^2 i - 4) \frac{1 + \frac{3}{2} e^2}{(1 - e^2)^2}$$

$$f_6 = \frac{7\sqrt{65}}{64} \left(\frac{R_e}{a}\right)^4 (8 - 36\sin^2 i + 33\sin^4 i) \frac{1 + 5e^2 + \frac{15}{8}e^4}{(1 - e^2)^4}$$

$a$ ,  $i$ , and  $c$  are the semi-major axis, inclination, and eccentricity of the satellite's orbit, and  $n$  is the satellite's mean angular velocity. For I.AGEOS 1,  $f_4 = 0.496$ ,  $f_6 = 0.129$ , and  $f_8 = 0.009$  [Cheng *et al.*, 1989]. Thus, the desired linear combination coefficients are  $a_4 \approx f_4$ ,  $a_6 \approx f_6$  and  $a_8 \approx f_8$ .

Using the above values for the linear combination coefficients  $a_4$ ,  $a_6$  and  $a_8$ , we linearly combine the even degree zonal atmospheric pressure-induced gravitational field coefficients from the NMC global pressure data for both the NIB and IB models. As before, the low frequency components having periods longer than 2 years are removed (see Figure 3 and Table 2 for the period 1984 to 1992). The formation of the linear combination of even degree zonal atmospheric pressure-induced gravitational field coefficients does improve the overall fit to the observations for both the NIB and IB models. The correlation coefficients between the modeled NMC pressure and observed I.AGEOS 1 results increase from 0.64 to 0.75 and 0.68 to 0.73 for the NIB and IB models, respectively (also compare Figures 1 and 3). At the annual period, the IB model is in closer agreement with the observations than the NIB model, agreeing in amplitude to within one  $\sigma$  and in phase to within two  $\sigma$ . But at the semi-annual period, neither the IB or NIB models agree with the observations.

Table 3: Correlation analysis (1 984-1 992)

$C_{20}$ only		$C_{even}$	
NIB 0.64 (0.424)	1130.68 (0.424)	NIB 0.75 (0.424)	1110.73 (0.424)

The number (0.424) in parenthesis represents the 99% significance level for zero correlation series with 36 samples. This value (0.424) is calculated from *t*-test for product moment correlation with  $N=36$ . Due to the filtering, the monthly estimates are correlated within the interval of 3 months. Thus the number of independent estimates is reduced from 108 to 36, which is taken into account.

Contributions from all geophysical mechanisms that can be expected to produce detectable signals should be considered when searching for the cause of the deficit at the semi-annual period. The principal non-atmospheric candidates for this deficit are likely to be ocean tidal and non-tidal mass redistributions, groundwater storage, and ice sheet volume changes. The deformation of the solid Earth due to seasonal variations in spin rate creates changes in the even degree zonal gravitational field coefficients at the  $10^{-12}$  level, which is too small to account for the above deficit. Table 2 gives the modeled contributions of seasonal ocean tidal and groundwater storage variations to the Earth's gravitational field (in both cases the same linear combination of the even degree zonal coefficients are formed as was done above for the atmospheric pressure variations). Note that the listed sources are incomplete; some potentially important contributors, such as wind-driven oceanic mass redistribution, are not included here due to a lack of published results.

At the semi-annual period, the ocean tides are expected to make a significant contribution. On seasonal and longer time scales, the oceanic response to tidal perturbation forces is likely to be close to equilibrium [Proudman, 1960; Carton and Wahr, 1986; Dickman, 1989]; dynamical models indicate that the discrepancies from equilibrium for the  $S_a$  and  $S_{sa}$  tides are very small [Dickman, 1989]. Schwiderski's tide model is constrained by tide gauge data, which include the effects from all perturbation sources [Schwiderski, 1980]. In particular, on seasonal time scales the variations of the atmospheric pressure, wind-driven currents, and probably the recycling of groundwater also enter the tide gauge data, thereby contaminating Schwiderski's  $S_a$  and  $S_{sa}$  results through hydrodynamic propagation. Similarly, satellite-geodesy derived ocean tide models [Christodoulidis et al., 1988] also contain the effects from mass variations of the atmosphere and groundwater. Since our aim is to model the ocean tidal contribution to the LAGEOS-observed even combination of gravitational field coefficients, we calculate the  $S_a$  and  $S_{sa}$  ocean tidal



contributions using the grid values of admittance. for long-period self-consistent equilibrium ocean tides from *Ray and Cartwright [1994]*. The effect on the annual component is found to be quite small (1-3% of the observed amplitude); while the impact is much greater on the semi-annual component (nearly 60% of the observed amplitude). With atmospheric pressure alone, only 30-45% of the observed semi-annual amplitude is accounted for; while when the ocean tidal effect is included, the amplitude and phase for ocean tide plus atmospheric pressure (for both the IB and NIB cases) are in agreement with the observations to within one  $\sigma$ .

The residual formed by subtracting from the observations the modeled effects of ocean tides and atmospheric pressure fluctuations is much smaller than the modeled effect of variations in groundwater storage. This suggests that either the effects of groundwater storage are being overestimated, or that some other geophysical mechanism is making a compensating contribution to the observed seasonal variations in the even linear combination of zonal gravitational field coefficients. A main goal of the Global Energy and Water Cycle Experiment (GEWEX; *Chahine, 1992*) program is to gain an improved understanding of the Earth's hydrological cycle. Thus, improved estimates of groundwater storage can be expected in the future. Other sources of geophysical excitation, such as the wind-driven oceanic mass redistribution, also remain to be studied. In addition, one cannot eliminate the possibility of incompleteness in the satellite perturbation force model, errors in the atmospheric pressure data, and deviations from equilibrium of the ocean tides, that would also contribute to these apparent residuals.

*Acknowledgments.* We gratefully acknowledge the Space Geodesy Branch at Goddard Space Flight Center for providing us with the GEODYN software package and the LAGEOS normal point data. We also thank 't'. Van Dam for providing the NMC atmospheric pressure data, R. D. Ray for providing the self-consistent equilibrium ocean tidal admittance grid data, and M. K. Cheng, R. S. Nerem, D. Rowland, M. Torrence and M. Watkins for helpful discussions. The CRAY supercomputer used in this investigation was provided by funding from the NASA offices of Mission to Planet Earth, Aeronautics, and Space Science. The plots were generated using the public domain Generic Mapping Tools (GMT) software [*Wessel and Smith, 1991*]. The work described in this paper was performed at the Jet Propulsion Laboratory, California Institute of Technology, under contract with the National Aeronautics and Space Administration,

## REFERENCES

- Carton, J. A., and J. M. Wahr, Modeling the Pole Tide and its Effect on the Earth's Rotation, *Geophys. J. R. astr. Soc.*, 84, 121-137, 1986.
- Chahine, M. T., The hydrological cycle and its influence on climate, *Nature*, **359**, 373--380, 1992,
- Chao, B. F., The geoid and Earth rotation, in *Geoid and its Geophysical Interpretations*, edited by P. Vanicek and N. '1'. Christou, pp. 285-298, CRC Press, Boca Raton, Florida, 1994.
- Ciao, B. F., and A. Y. Au, Atmospheric Excitation of the Earth's Annual Wobble, *J. Geophys. Res.*, 96,6577 -6582., 1991.
- Chao, B. F., and W. P. O' Connor, Global Surface-Water-Induced Seasonal Variations in the Earth's Rotation and Gravitational Field, *Geophys. J.*, 94,263-270, 1988.
- Cheng, M. K., C. K. Shum, R. J. Eanes, B. E. Schutz, and B. D. Tapley, Temporal Variation in Low Degree Zonal 11 harmonics from Starlet to Orbit Analysis, *Geophys. Res. Lett.*, 16,393-396, 1989.
- Christodoulidis, D. C., D. E. Smith, R. G. Williamson, and S. M. Klosko, Observed Tidal Breaking in the Earth/Moon/Sun System, *J. Geophys. Res.*, 93, 6212-6236, 1988.
- Dickman, S. R., A Complete Spherical Harmonic Approach to Luni-Solar Tides, *Geophys. J. Int.*, 99, 457-468, 1989.
- Dong, D., and Y. Bock, Global Positioning System Network Analysis with Phase Ambiguity Resolution Applied to Crustal Deformation Studies in California, *J. Geophys. Res.*, 94, No. B4, 3949-3966, 1989.
- Eanes, R. J., and M. M. Watkins, Temporal Variability of Earth's Gravitational Field from Satellite Laser Ranging Observations, *XX General Assembly of the IUGG, IAG Symp. No. 3*, Vienna, Austria, August 1991.
- Farrel, W. E., Deformation of the Earth by SLIJ'face Loads, *Rev. Geophys.*, 10, 761-797, 1972.
- Gegout, P., and A. Cazenave, Geodynamic parameters derived from 7 years of laser data on Lagos, *Geophys. Res. Lett.*, **18**, 1739-1742, 1991.

- Gegout, P., and A. Cazenave, Temporal Variations of the Earth Gravity Field for 1985-1989 Derived from LAGEOS, *Geophys. J. Int.*, 114, 347-359, 1993.
- Gross, R. S., A combination of Earth orientation data: SPAC192, in IERS'77 Technical Note 14: *Earth Orientation, Reference Frames and Atmospheric Excitation Functions Submitted for the 1992 IERS Annual Report*, edited by P. Charlot, pp. C 1-C%, Observatoire de Paris, Paris, France, 1993.
- Gutierrez., R., and C.R. Wilson, Seasonal Air and Water Mass Redistribution Effects on LAGEOS and Starlette, *Geophys. Res. Lett.*, 14, 929-932, 1987.
- Huang, C., J. C. Ries, B.D. Tapley, and M.M. Watkins, Relativistic Effects for Near-Altitude Satellite Orbit Determination, *Cel. Mech. Dyn. Astro.*, 48, 167-185, 1990.
- Kaula, W. M., Theory of Satellite Geodesy, 124 pp., Blaisdell, Waltham, Mass., 1966.
- Nerem, R. S., B. F. Chao, A. Y. Au, J. C. Chan, S. M. Klosko, N. K. Pavlis, and R. G. Williamson, Temporal Variations of the Earth's Gravitational Field from Satellite Laser Ranging to LAGEOS, *Geophys. Res. Lett.*, 20, 595-598, 1993.
- Nerem, R. S., S. M. Klosko, N. K. Pavlis, R. G. Williamson, and E. C. Pavlis, Atmospheric Mass Redistribution at Tidal Frequencies from Temporal Geopotential Variations Observed by SLR, *EOS*, 75, 112, 1994a.
- Nerem, R. S., F. J. Lerch, J. A. Marshall, E. C. Pavlis, B. H. Putney, B. D. Tapley, R. J. Hanes, J. C. Ries, B. E. Schutz, C. K. Shum, M. M. Watkins, J. C. Chan, S. M. Klosko, S. B. Luthcke, G. B. Pate], N. K. Pavlis, R. G. Williamson, R. H. Rapp, R. Biancale, and F. Nouel, Gravity Model Development for TOPEX/Poseidon: Joint Gravity Models 1 and 2, submitted to *J. Geophys. Res.*, 1994b.
- Proudman, J., The condition that a long-period tide should follow the equilibrium-law, *Geophys. J. Roy. astr. Soc.*, 3, 244-249, 1960.
- Ray, R. D., and D. E. Cartwright, Satellite altimeter observations of the M<sub>2</sub> and M<sub>4</sub> ocean tides, with simultaneous orbit corrections, in *Gravimetry and Space Techniques Applied to Geodynamics and Ocean Dynamics*, edited by B. E. Schutz, A. Anderson, C. Froidevaux, and M. Parke, pp. 69--78, American Geophysical Union Geophysical Monograph 82, UGG Volume 17, Washington, D.C., 1994.

- Rubincam, D. P., Postglacial rebound observed by LAGEOS and the Effective Viscosity of the Lower Mantle, *J. Geophys. Res.*, 89, 1077-1087, 1984,
- Rubincam, D. P., Yakovsky Thermal Drag on LAGEOS, *J. Geophys. Res.*, 93, 13805-13810, 1988,
- Scherneck, H.-G, A Parameterized Solid Earth Tide Model and Ocean Tide Loading Effects for Global Geodetic Baseline Measurements, *Geophys. J. Int.*, 106, 677-694, 1991.
- Schwiderski, E. W., Ocean tides I: Global Ocean Tides Equations, *Mar. Geod.*, 3, 161-217, 1980.
- Trupin, A., and J. Wahr, Spectroscopic Analysis of Global Tide Gauge Sea-Level Data, *Geophys. J. Int.*, 100, 441-453, 1990.
- Wessel, P., and W. H.F. Smith, Free software. helps map and display data, *Eos, Trans, AGU*, 72, 441, 1991
- Yoder, C.F., J. G. Williams, J. O. Dickey, B.B. Schutz, R. J. Eanes, and B.D. Tapley, Secular Variations of the Earth's Gravitational Harmonic  $J_2$  Coefficient from LAGEOS and Non-Tidal Acceleration On Earth Rotation, *Nature*, 303, 757-762, 1983,

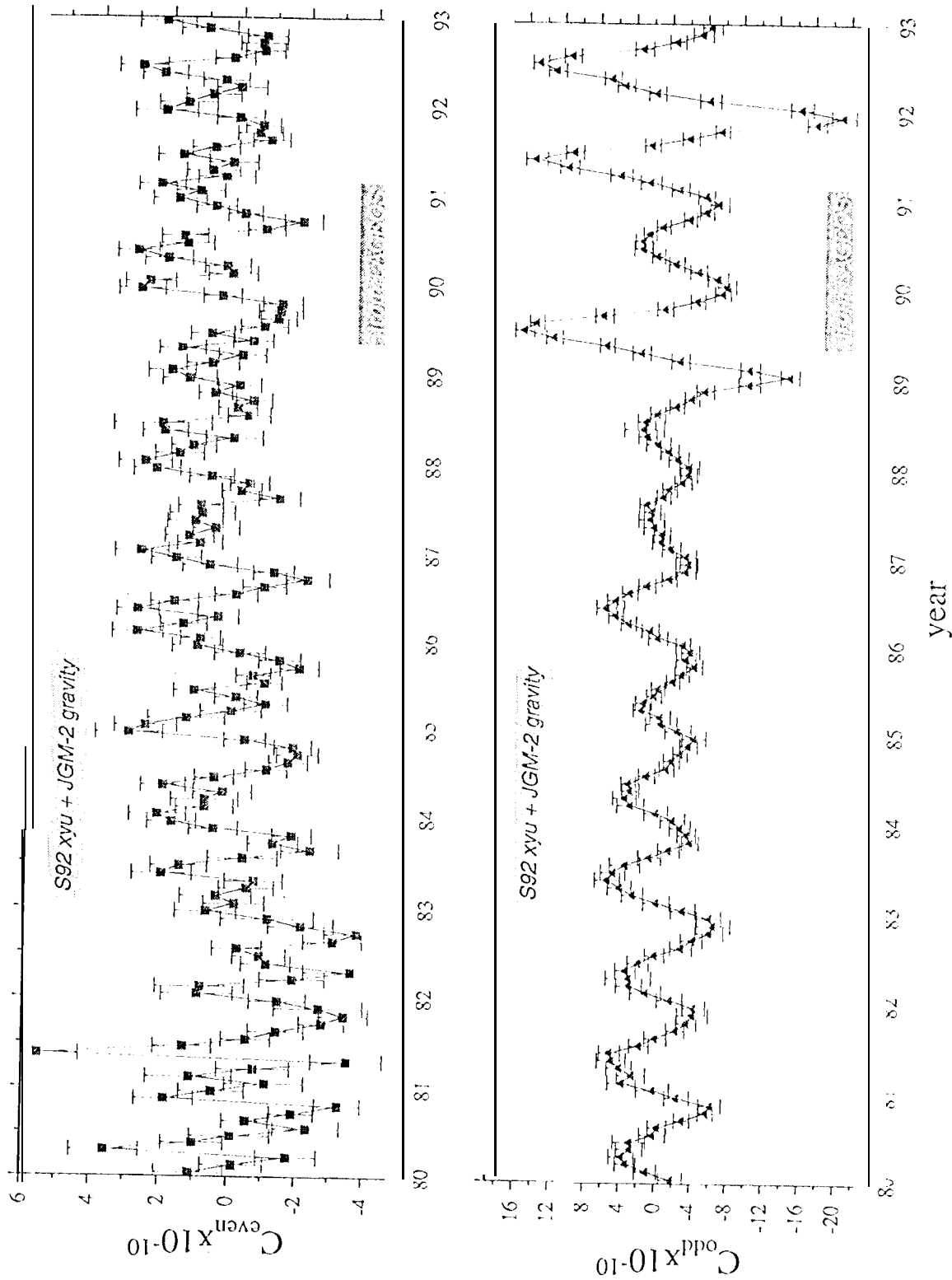


Figure 1: Monthly  $C^{even}$ ,  $C^{odd}$  linear combination of gravitational coefficients from Jan. 1980 to Dec. 1992 recovered from LAGEOS I SLR data. The error bar represents a  $1\sigma$  formal uncertainty. The mean values of the  $C^{even}$ ,  $C^{odd}$  have been removed in the plot.

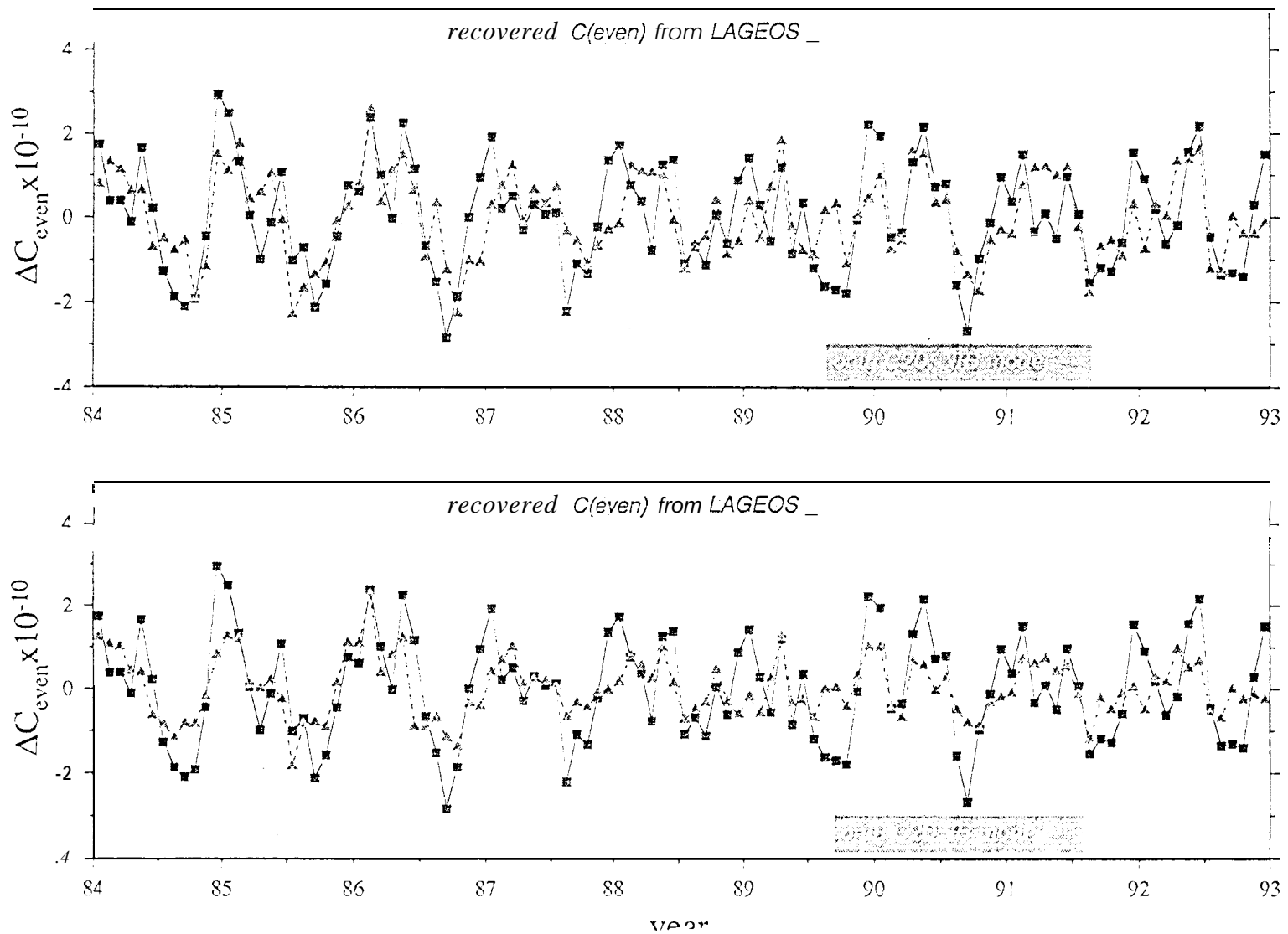


Figure 2: (a) Variations of monthly  $C_{20}$  recovered from LAGEOS I SLR data (solid line), and the variations of monthly  $C_{20}$  calculated from NMC atmospheric surface pressure data with non-inverted-barometer (SIB) model (dashed line). The variations with periods longer than two years have been removed from both series. (b) Same as (a) except the dashed line represents the variations of monthly  $C_{20}$  calculated from NMC atmospheric surface pressure data with inverted-barometer (IB) model.

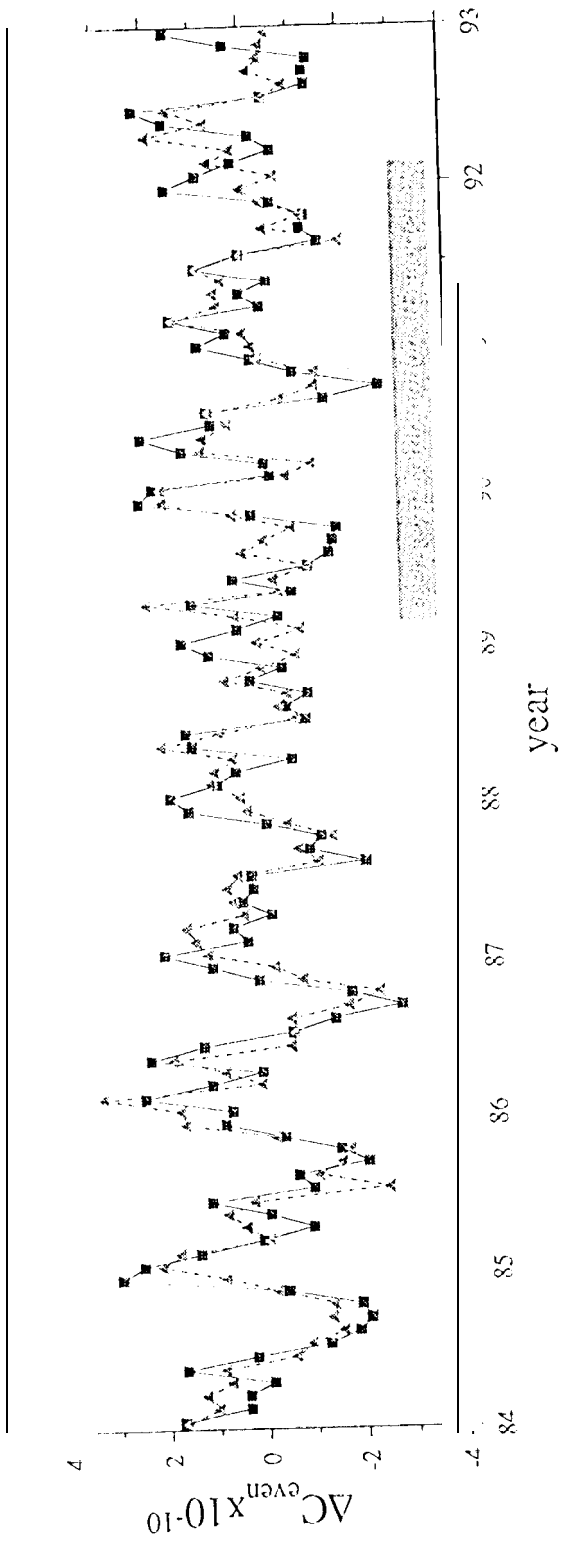
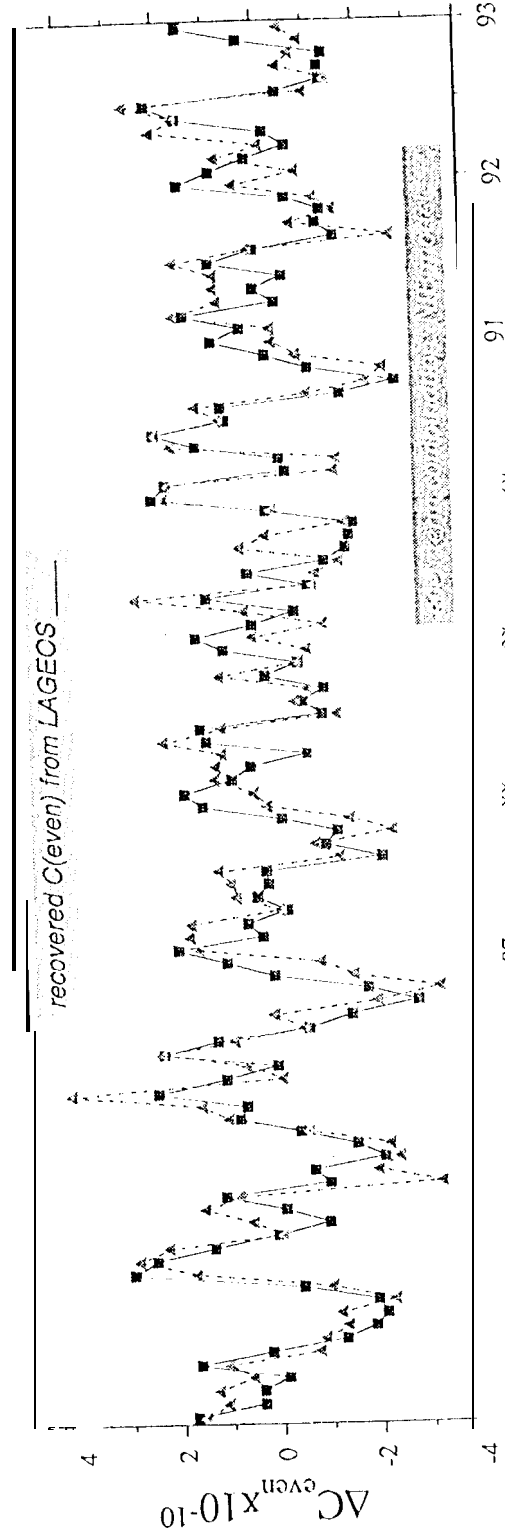


Figure 3: (a) Variations of monthly  $C_{even}$  recovered from LAGEOS I SLR data (solid line) and the variations of monthly  $C_{even}$  calculated from NMC atmospheric surface pressure data with non-inverted-barometer (NIB) model (dashed line). The variations with periods longer than two years have been removed from both series. (b) Same as (a) except the dashed line represents the variations of monthly  $C_{even}$  calculated from NMC atmospheric surface pressure data with inverted-barometer (IB) model.